

Research Article

A Comparative Study of the Skeletal Development of *Epinephelus fuscoguttatus* (♀) and *E. tukula* (♂) Hybrid Progeny and *E. fuscoguttatus*

Xinyi Wang,^{1,2} Yongsheng Tian ,^{2,3} Shuai Chen,^{1,2} Linlin Li,^{2,4} Pengfei Duan,^{1,2} Zhongtong Li,^{2,3} Linna Wang,^{2,3} Yang Liu,^{2,3} Qingbin Wang,⁵ Wensheng Li,⁵ and Xia Zhao⁵

¹College of Fishers and Life Sciences, Shanghai Ocean University, Shanghai 201306, China

²Key Laboratory of Sustainable Development of Marine Fisheries, Ministry of Agriculture and Rural Affairs, Yellow Sea Fisheries Research Institute, Chinese Academy of Fishery Sciences, Qingdao 266071, China

³Laboratory for Marine Fisheries Science and Food Production Processes, Pilot National Laboratory for Marine Science and Technology (Qingdao), Qingdao 266071, China

⁴Chinese Academy of Agricultural Sciences, Beijing 100081, China

⁵Mingbo Aquatic Co. Ltd, Laizhou 261400, China

Correspondence should be addressed to Yongsheng Tian; tianys@ysfri.ac.cn

Received 24 August 2022; Revised 17 October 2022; Accepted 6 January 2023; Published 21 February 2023

Academic Editor: Zhitao Qi

Copyright © 2023 Xinyi Wang et al. This is an open access article distributed under the Creative Commons Attribution License, which permits unrestricted use, distribution, and reproduction in any medium, provided the original work is properly cited.

As a new breed of grouper hybrid breeding, EFT has the advantages of delicious flesh, fast growth, and high deformity rate. We explored the metamorphosis and skeletal development of *Epinephelus fuscoguttatus* and hybrids (EFT) of *E. fuscoguttatus* (♀) and *E. tukula* (♂). EFT grew slightly slower than *E. fuscoguttatus* during the larval period but grew faster during the juvenile period. The sequences of skeletal development were similar in EFT and *E. fuscoguttatus*. Newly hatched larvae did not have skeletons until 5 days after hatching (DAH) when head cartilage started to develop and complete at 43 days later. The vertebral column started to develop at 11 DAH and was completed at 38 DAH. Pectoral fin development began at 5 DAH and ossification was completed at 48 DAH in EFT and at 43 DAH in *E. fuscoguttatus*. Anal fin development started at 11 DAH and ossification was completed earlier in EFT than in *E. fuscoguttatus*. The caudal fins of the two groupers developed at 8 DAH and ossified earlier in EFT than in *E. fuscoguttatus*. In contrast, *E. fuscoguttatus* had one additional epural than EFT. These results provide important basic biological data for the growth and skeletal development of pure and hybrid grouper.

1. Introduction

Epinephelus fuscoguttatus and *E. tukula* are groupers belonging to the *Perciformes*, *Serranidae*, and *Epinephelinae*. *E. fuscoguttatus* has delicious flesh and a high market value; however, its growth rate is slow and its feeding cycle is long. It is often used as the female parent of hybrid groupers owing to its strong disease resistance. *E. tukula* is a giant grouper, distributed in the southern waters of China; it is not widely cultured, and the breeding resources are mainly derived from wild fishing. We have used frozen sperm of *E. tukula* to fertilize *E. fuscoguttatus* eggs, overcoming reproductive

isolation, to obtain hybrids (referred to as EFT). EFT has high survival rate, low malformation rate, and fast growth rate. It has an obvious hybridization advantage. Research on EFT to date has focused on its growth and metamorphosis [1], morphological properties [2], genetic diversity [3], hypoxia tolerance [4], and karyotype [5]. The above-given studies also indicated that EFT has rich genetic diversity and low oxygen tolerance. Skeletal development has not been compared between EFT and *E. fuscoguttatus*.

The bones of fish are divided into the central axial skeleton, including the cephalic and vertebral column, and the appendage skeleton, including the even-fin skeleton and

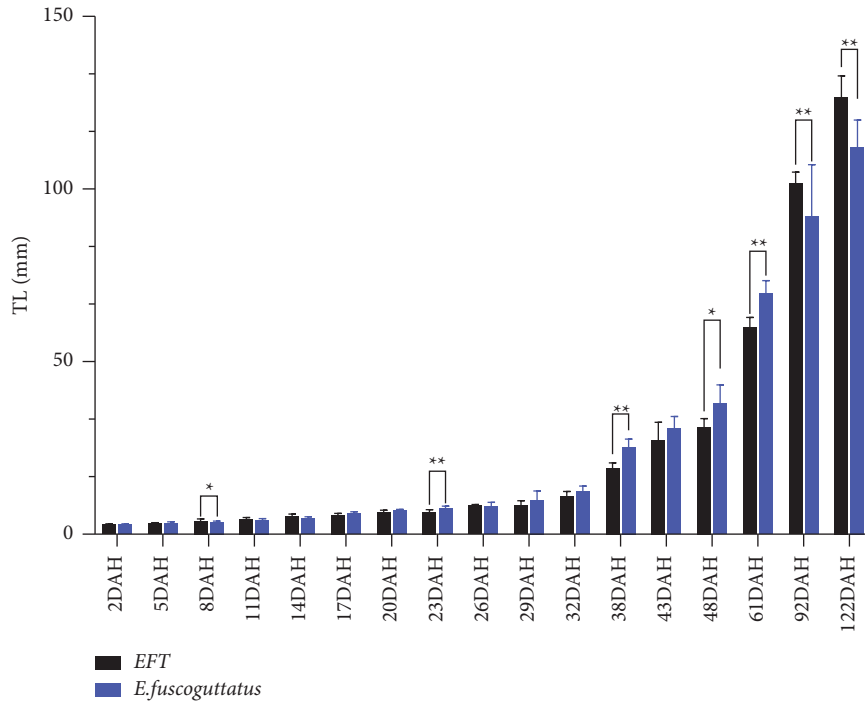


FIGURE 1: Total length of EFT and *E. fuscoguttatus*. ** $P < 0.01$, * $P < 0.05$.

odd-fin skeleton [6]. Skeletal development is essential for fry rearing during feeding. The skeleton not only supports the fish body but also protects the internal organs and coordinates movements. In the processes of fish growth and metamorphosis, an initial period of allometric growth of survival-related bones helps to reduce fish mortality and improve survival [7]. In addition, abnormal bone development can result in difficult movement, slow growth, and high rates of mortality.

In this study, bone development was observed in *E. fuscoguttatus* and EFT by the dual staining of hard bone and cartilage, and a comparative analysis was performed to determine the nutritional and environmental factors necessary for growth and metamorphosis and to explore the growth-related advantages of EFT as a hybrid grouper.

2. Materials and Methods

2.1. Ethic Statement. This study was approved by the Animal Care and Use Committee of the Yellow Sea Fisheries Research Institute [YSFRI-2022027].

2.2. Egg Fertilization, Hatching, and Fry Cultivation. EFT was obtained by the artificial fertilization of *E. fuscoguttatus* eggs with the thawed frozen sperm of *E. tukula*. The embryos of the two species of grouper were obtained from Laizhou Mingbo Aquatic Products Co., Ltd., (Shandong Province, China). EFT and *E. fuscoguttatus* were cultured in circulating water environments with a water temperature of 28°C, salinity of 30‰, and 6 mg/L dissolved oxygen. The ponds were circular with a volume of 40 m³. Before 2 days after hatching

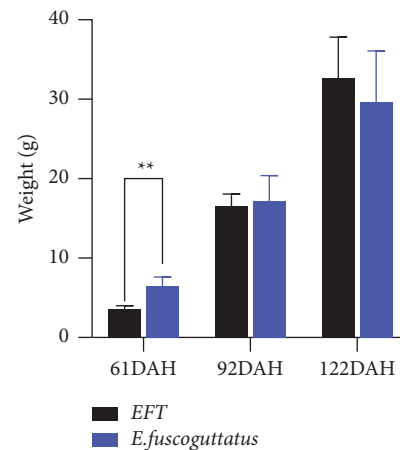


FIGURE 2: Weight of EFT and *E. fuscoguttatus*.

(DAH), the yolk sac provides nutrients to the larvae. From 2 to 5 DAH, fish were fed SS rotifers (8–10 individuals mL⁻¹). From 5 to 10 DAH, fish were fed L-rotifers (10–15 individuals mL⁻¹). From 10 to 16 DAH, fish were fed nauplii of *Artemia* (0.5–2 individuals mL⁻¹). From 16 to 24 DAH, fish were fed adult *Artemia* (0.5–2 individuals mL⁻¹), followed by a gradual transition to pellets. The feeding amount was adjusted according to the growth of the groupers.

2.3. Sample Collection and Treatment. Ten EFT and ten *E. fuscoguttatus* embryos were obtained for observation every 3 days. After observing the morphology of samples under an inverted biomicroscope and inverted anatomical microscope, the samples were anesthetized with MS-222.

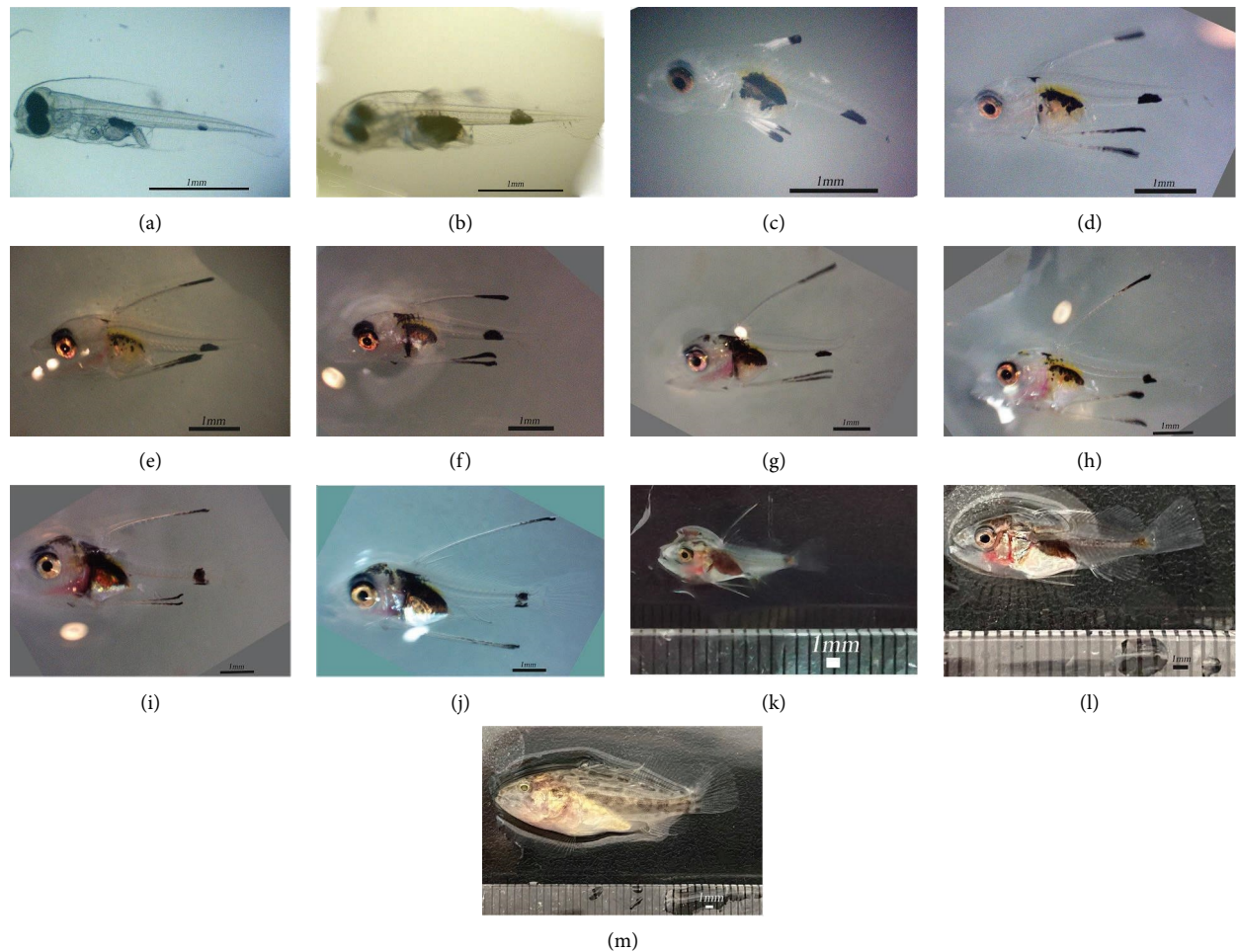


FIGURE 3: Postembryonic development of EFT. (a) 2 DAH (0.28 ± 0.02 mm TL); (b) 5 DAH (0.32 ± 0.02 mm TL); (c) 8 DAH (0.4 ± 0.04 mm TL); (d) 11 DAH (0.44 ± 0.04 mm TL); (e) 14 DAH (0.5 ± 0.08 mm TL); (f) 17 DAH (0.56 ± 0.04 mm TL); (g) 20 DAH (0.64 ± 0.05 mm TL); (h) 23 DAH (0.65 ± 0.06 mm TL); (i) 26 DAH (0.83 ± 0.04 mm TL); (j) 29 DAH (0.84 ± 0.12 mm TL); (k) 32 DAH (1.09 ± 0.15 mm TL); (l) 38 DAH (1.92 ± 0.14 mm TL); (m) 43 DAH (2.72 ± 0.46 mm TL).

2.4. Growth Measurement. Images of samples were obtained after observation under a microscope. Then, the total length of each sample was determined.

At the end of metamorphosis, 30 *E. fuscoguttatus* and 30 EFT were randomly selected each month for three consecutive months. Samples were weighed and the total length and body length were determined.

2.5. Observation of Skeletal Development. Samples of both fish were stained using previously described bone staining methods [8, 9]. Samples were fixed in 10% formalin for 24 h and then washed with distilled water for 24 h. Next, they were stained with Alcian blue staining solution for cartilage detection until the fish body turned medium blue. Samples were transferred to 95% ethanol for 2-3 h and then washed sequentially in 75%, 40%, and 15% alcohol gradients for 2-3 h per wash. Samples were immersed in distilled water until the fish sank and then placed in a borax-trypsin solution for digestion. When the muscle digestion was completed and the fish body appeared transparent state, the hard bone was stained with alizarin red dye until samples turned red.

Samples were washed with 0.5% KOH-glycerol solution and three 0.5% KOH-glycerol solutions (3:1, 1:1, and 1:3) for 24 h each until the melanin was removed (each solution included two drops of 3% H_2O_2). Finally, the samples were stored in glycerol-containing thymol and skeletal development was observed under an inverted anatomical microscope.

The morphological characteristics and skeletal development of EFT and *E. fuscoguttatus* were observed using the DSY2000X inverted biomicroscope (Chongqing Photoelectric Instrument Co., Ltd.) and SZ810 inverted anatomical microscope (Chongqing Aoter Optical Microscope Co., Ltd.). Image View was used to measure fish lengths. Images were annotated using Adobe Photoshop CS6.

3. Results

3.1. Postembryonic Development of EFT and *E. fuscoguttatus*. The total lengths and weights of *E. fuscoguttatus* and EFT are shown in Figures 1 and 2, respectively.

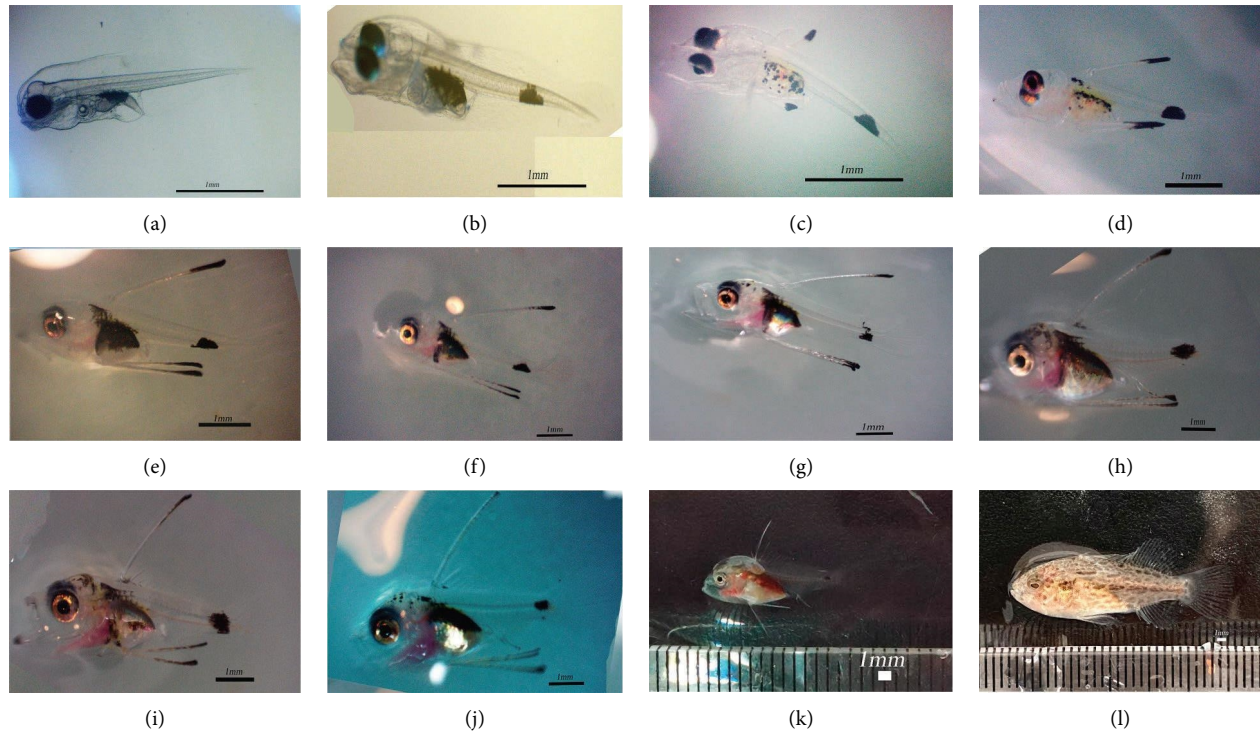


FIGURE 4: Postembryonic development of *E. fuscoguttatus*. (a) 2 DAH (2.85 ± 0.1 mm TL); (b) 5 DAH (3.21 ± 0.37 mm TL); (c) 8 DAH (3.61 ± 0.22 mm TL); (d) 11 DAH (4.21 ± 0.40 mm TL); (e) 14 DAH (4.76 ± 0.28 mm TL); (f) 17 DAH (6.00 ± 0.47 mm TL); (g) 20 DAH (6.85 ± 0.59 mm TL); (h) 23 DAH (7.59 ± 0.46 mm TL); (i) 26 DAH (8.07 ± 1.08 mm TL); (j) 29 DAH (9.99 ± 2.46 mm TL); (k) 32 DAH (12.38 ± 1.53 mm TL); (l) 38 DAH (25.16 ± 2.19 mm TL).

At 2–20 days, the total lengths of EFT and *E. fuscoguttatus* were similar. Thereafter, *E. fuscoguttatus* had a longer overall length than that of EFT. After 61 days, the gap between the full length of *E. fuscoguttatus* and EFT narrowed gradually. At 122 days, the total lengths of EFT (126.47 ± 6.02 mm TL) were significantly longer than that of *E. fuscoguttatus* (111.92 ± 7.67 mm TL).

At 61 DAH, the weight of the EFT was significantly less than that of *E. fuscoguttatus*. At 92 DAH, the weight gap between EFT and *E. fuscoguttatus* narrowed. At 122 DAH, the weight of EFT was not significantly different from that of *E. fuscoguttatus*, but EFT weighs more than *E. fuscoguttatus*.

3.1.1. Postembryonic Development of *E. fuscoguttatus*. At 2–5 DAH, the egg yolk sac of *E. fuscoguttatus* was continually consumed, the oil ball became smaller, and an oral fissure was detected. The digestive tract became thicker, and melanin deposition was observed in the upper part of the digestive tract. The eyeball was completely black, the auditory sac behind the eye was obviously visible, and the bone in the jaw became visible. The fin folds on both sides of the anterior tail were slightly concave, and there was a small amount of melanin deposition in one-third of the body at the front of the tail (Figures 3(a) and 3(b)).

At 6–23 DAH, the eyeball became bright and the pupil was clearly visible, the melanin of the internal organ mass

decreased gradually, and the area where the melanin was receding appeared silvery-white. The heart area and gills appeared bright red. At 26 DAH, a bright red blood vessel along the spine could be seen and the second dorsal and ventral spines grew. As the fish grew, the second dorsal and ventral spines continued to elongate up to one-half the length of the body, with melanin deposition at the ends of the fin lepidotrichia. The fin folds at the front of the tail continued to recede inward to the narrowest point, the vertebral column appeared segmented, the end of the spine was upturned, and the fin lepidotrichia could be seen in the tail. At 17 DAH, a large number of dead *E. fuscoguttatus* larvae were observed, with high rates of cannibalism between groups and a survival rate of only 30% (Figures 3(c)–3(g)).

At 24–48 DAH, the orbit deepened and a fold formed on the skin around the eyes. The second dorsal and ventral spines began to contract, the melanin at the end gradually receded, the dorsal and ventral fins were clearly visible (except for the contracted fin lepidotrichia), and the pectoral and caudal fins were clearly visible. At 38 DAH, the body of *E. fuscoguttatus* was no longer completely transparent, and the body surface had a pattern, with scales covering the body surface. At 43 DAH, the fish body was completely opaque, and the pattern on the body surface was roughly similar to that of adult fish (Figures 3(h)–3(l)).

At 61 DAH, *E. fuscoguttatus* was 6.9 ± 0.4 cm in total length and weighed 6.4 ± 1.1 g. At 92 DAH, individuals were

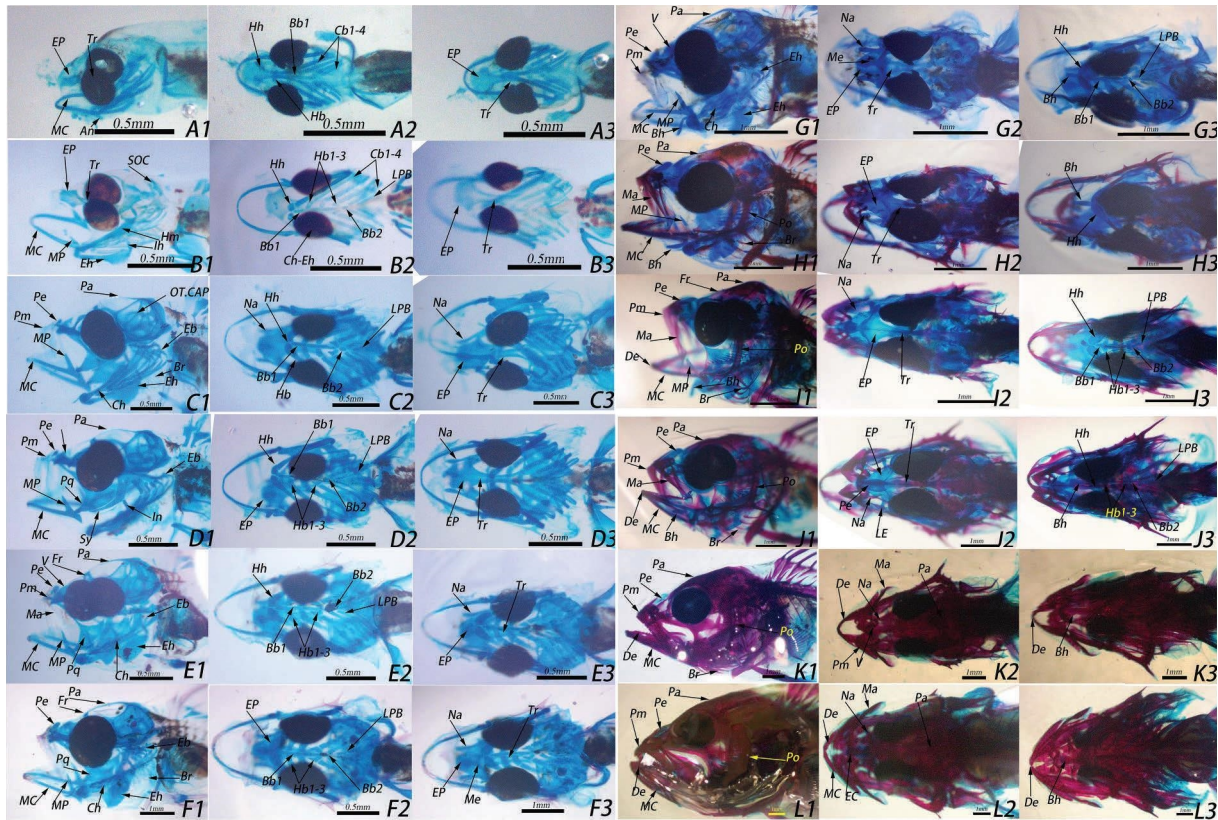


FIGURE 5: Cephalic skeleton development of EFTA1-L1(lateralview) A2-L2(dorsalview) A3-L3(ventralview). (a) 5 DAH (3.2 ± 0.17 mm TL); (b) 8 DAH (3.97 ± 0.4 mm TL); (c) 11 DAH (4.43 ± 0.41 mm TL); (d) 14 DAH (5.04 ± 0.77 mm TL); (e) 17 DAH (5.61 ± 0.41 mm TL); (f) 20 DAH (6.45 ± 0.48 mm TL); (g) 23 DAH (6.53 ± 0.63 mm TL); (h) 26 DAH (8.34 ± 0.44 mm TL); (i) 29 DAH (8.40 ± 1.2 mm TL); (j) 32 DAH (10.87 ± 1.49 mm TL); (k) 38 DAH (19.18 ± 1.40 mm TL); (l) 43 DAH (27.21 ± 4.6 mm TL). Abbreviations are as follows: an: angular; Bh: basihyal; Br: branchiostegal; Bb1: basibranchial cartilages1; Bb2: basibranchial cartilages2; Ch: ceratohyal; Cb: ceratobranchial; De: dentary; EP: ethmoid plate; EC: ethmoid cartilage; Eh: epihyal; Fr: frontal; Hh: hypohyal; Hb: hypobranchial; Ih: interhyal; LPB: lower pharyngeal bone; LE: lateral ethmoid; MC: Meckel's cartilage; Ma: maxillary; Na: nasal; MP: mediadorsal; Pe: proethmoid; Pq: palatoquadrate; Pa: parietal; Po: preopercle; Pm: premaxillary; SOC: supraoccipital; Sy: symplectic; Tr: trabeculae; V: vomer.

9.2 ± 1.4 cm in total length and weighed 17.1 ± 3.2 g. At 122 DAH, the total length was 11.2 ± 0.8 cm and the weight was 29.7 ± 6.3 g.

3.1.2. Postembryonic Development of EFT. At 2–5 DAH, there were no observable differences in development between EFT and *E. fuscoguttatus* (Figures 4(a) and 4(b)).

At 6–20 DAH, the pupil was clearly visible and the visceral mass melanin receded from the abdomen to the back and was covered in silvery white. The vertebral column was not cylindrical, the neural arch and hemal arch were visible, and the end of the vertebral column were upturned. The second dorsal and ventral spines were elongated, barbs could be seen on the spines of the fins, and melanin was deposited at the ends. The front of the visceral mass, gills, and heart was bright red. The number of EFT deaths was low, and the survival rate was 80% (Figures 4(c)–4(h)).

At 21–48 DAH, the development of EFT was similar to that of *E. fuscoguttatus*, other than an elongated the body of EFT. At 43 DAH, the black pattern appeared on the surface of the body. At 48 DAH, the fish body was completely

opaque and the dorsal fin, abdominal fin, anal fin, caudal fin, and pectoral fin were clearly visible. The body surface pattern was not substantially different from that of adult fish (Figure 4(i)).

At 61 DAH, EFT was 6.0 ± 0.3 cm in total length and 3.5 ± 0.5 g in weight. At 92 DAH, the total length was 10.2 ± 0.3 cm and the weight was 16.4 ± 1.6 g. At 122 DAH, the total length was 12.6 ± 0.6 cm and the weight was 32.7 ± 5.1 g.

3.2. Axial Skeletal Development of *E. fuscoguttatus* and EFT

3.2.1. Development of the Cranium. At 2 DAH, juvenile fish lacked head cartilage. At 5 DAH (Figures 5(a) and 6(a)), larvae in both groups did not differ substantially, showing the development of the ethmoid plate, trabeculae, Michael's cartilage, four ceratobranchials, basibranchial cartilage, hypohyal, and hypobranchial. At 8 DAH (Figures 5(a) and 6(b)), both fish had a visible lower pharyngeal bone and supraoccipital, and basibranchial cartilage 2. In addition, in *E. fuscoguttatus*, nasal and palatoquadrate cartilage were detected. At 11 DAH (Figures 5(c) and 6(c)), two groupers

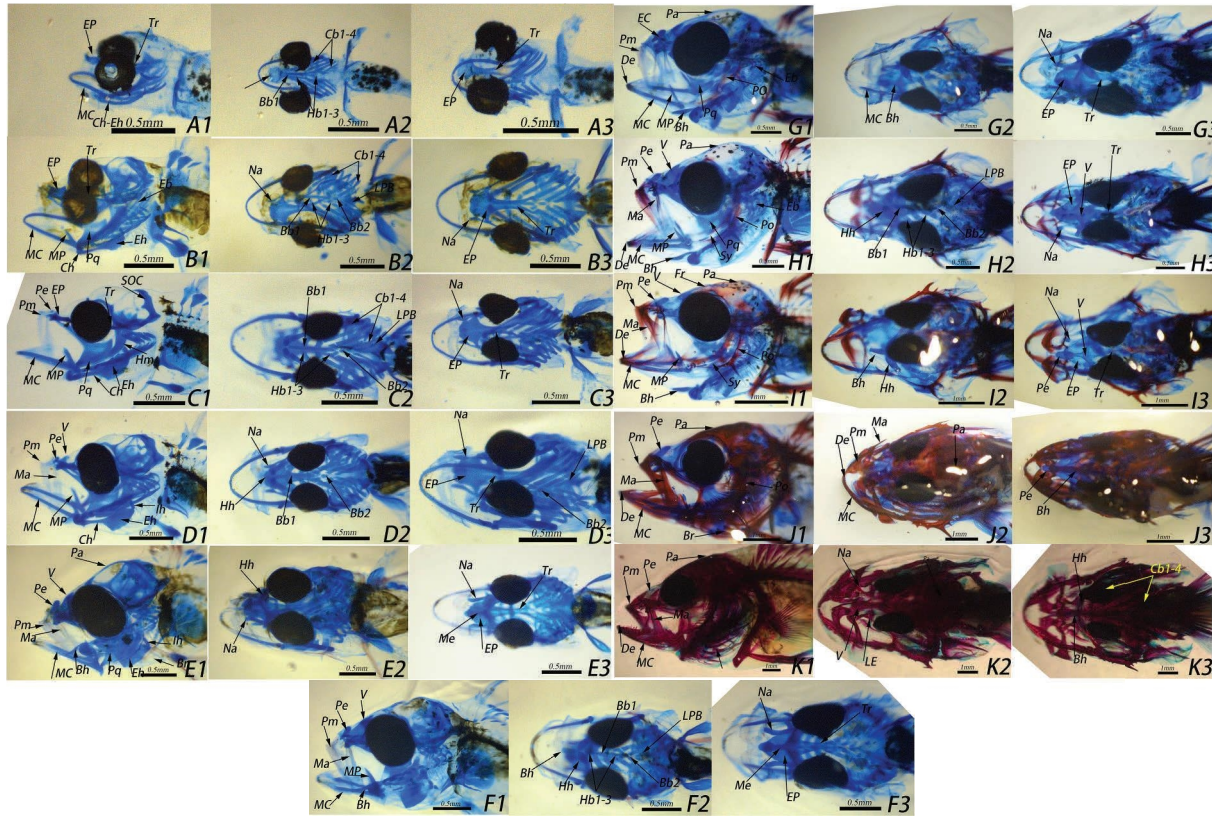


FIGURE 6: Cephalic skeleton development of *E. fuscoguttatus* A1-K1(lateralview) A2-K2(dorsalview) A3-K3(ventralview). (a) 2 DAH (2.85 ± 0.1 mm TL); (b) 5 DAH (3.21 ± 0.37 mm TL); (c) 8 DAH (3.61 ± 0.22 mm TL); (d) 11 DAH (4.21 ± 0.40 mm TL); (e) 14 DAH ($TL4.76 \pm 0.28$ mm); (f) 17 DAH (6.00 ± 0.47 mm TL); (g) 20 DAH (6.85 ± 0.59 mm TL); (h) 23 DAH (7.59 ± 0.46 mm TL); (i) 26 DAH (8.07 ± 1.08 mm TL); (j) 29 DAH (9.99 ± 2.46 mm TL); (k) 32 DAH (12.38 ± 1.53 mm TL). Abbreviations are as follows: An: angular; Bh: basihyal; Br: branchiostegal; Bb1: basibranchial cartilages1; Bb2: basibranchial cartilages2; Ch: ceratohyal; Cb: ceratobranchial; De: dentary; EP: ethmoid plate; EC: ethmoid cartilage; Eh: epihyal; Fr: frontal; Hh: hypohyal; Hb: hypobranchial; Ih: interhyal; LPB: lower pharyngeal bone; LE: lateral ethmoid; MC: Meckel's cartilage; Ma: maxillary; Na: nasal; MP: mediadorsal; Pe: proethmoid; Pq: palatoquadrate; Pa: parietal; Po: preopercle; Pm: premaxillary; SOC: supraoccipital; Sy: symplectic; Tr: trabeculae; V: vomer.

began to develop premaxilla and proethmoid, and the nasal and palatoquadrate cartilage of EFT began to appear. At 14–20 DAH (Figures 5(d)–5(f), 6(d)–6(f)), the vomer was developed and the maxillary began to ossify. At 23–29 DAH (Figures 5(g)–5(i), 6(g)–6(i)), the branchiostegal was visible, the palatoquadrate began to degenerate, the parietal, maxilla, premaxilla, and preopercular gradually ossified, and dentary appeared. At 32–48 DAH (Figures 5(j)–5(l), 6(j) and 6(k)), bone ossification in each part of the head was completed.

3.2.2. Development of the Vertebral Column. At 11 DAH (Figures 7(a) and 8(a)), the neural arch formed from the front of the back and the hemal arch formed from the front of the abdomen. At 17 DAH (Figures 7(c) and 8(c)), the neural arch and hemal arch were completely formed and the parapophysis was visible. Prior to this point, the two grouper species developed at approximately the same rate. At 20 DAH (Figure 7(d)), the vertebral column of EFT began to ossify, while this was observed as 23 DAH in *E. fuscoguttatus* (Figure 8(e)). At 29–32 DAH (Figures 7(g), 7(h), 8(g), and 8(h)), two species

of grouper had abdominal ribs and dorsal ribs. At 38 DAH (Figures 7(i) and 8(i)), EFT and *E. fuscoguttatus* vertebrae, neural arches, hemal arches, and parapophysis were completely ossified. When ossification was completed, both EFT and *E. fuscoguttatus* had 19 vertebrae.

3.3. Appendage Skeletal Development of *E. fuscoguttatus* and EFT

3.3.1. Development of the Pectoral Fin. At 5 DAH (Figure 9(a)), the EFT coracoid-scapula cartilage and fin plate were visible. At 6–26 DAH (Figures 9(b)–9(h)), the fin part gradually degenerated to form the proximal radius, while the distal radials were visible. At 26 DAH (Figure 9(h)), the pectoral fin was visible. At 48 DAH (Figure 9(m)), the pectoral fin was completely ossified.

In the development of the pectoral fin of *E. fuscoguttatus*, at 5 DAH (Figure 10(a)), coracoid-scapula cartilage was visible. At the 8 DAH (Figure 10(b)), fin plate and cleithrum appeared. At 9–17 DAH (Figures 10(c)–10(e)), part of the fin

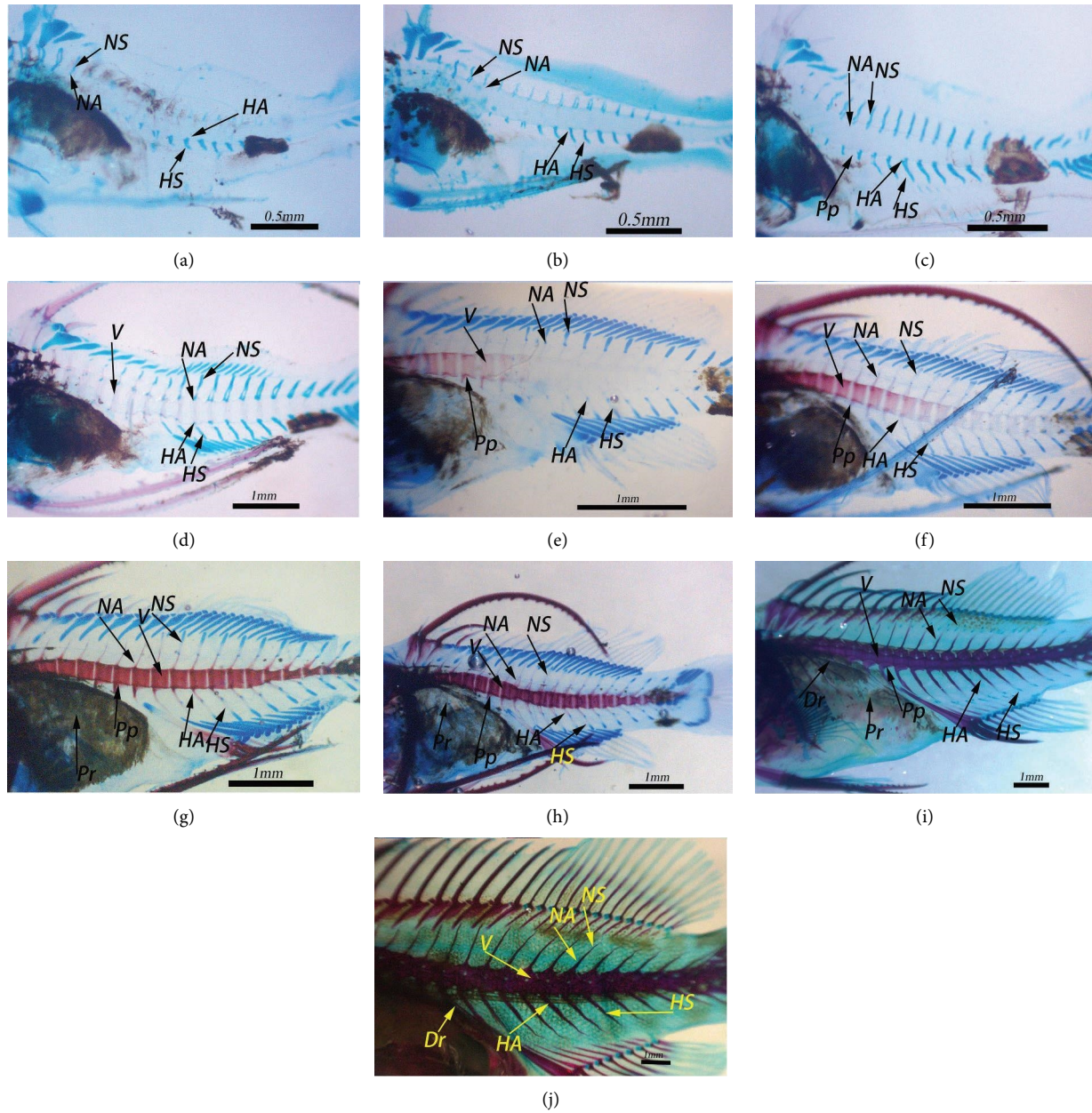


FIGURE 7: Vertebral column development of EFT. (a) 11 DAH (4.43 ± 0.41 mm TL); (b) 14 DAH (5.04 ± 0.77 mm TL); (c) 17 DAH (5.61 ± 0.41 mm TL); (d) 20 DAH (6.45 ± 0.48 mm TL); (e) 23 DAH (6.53 ± 0.63 mm TL); (f) 26 DAH (8.34 ± 0.44 mm TL); (g) 29 DAH (8.40 ± 1.2 mm TL); (h) 32 DAH (10.87 ± 1.49 mm TL); (i) 38 DAH (19.18 ± 1.40 mm TL); (j) 43 DAH (27.21 ± 4.6 mm TL). Abbreviations are as follows: Dr: dorsal rib; HS: heamal spine; HA: heamal arch; NA: neural arch; NS: neural spine; Pp: parapophysis; Pr: pleural rib; V: vertebral centra.

plate gradually degenerated to form proximal radials. At 20 DAH (Figure 10(f)), the pectoral fin was visible. At 21–43 DAH (Figures 10(g)–10(l)), ossification of the pectoral fin, cleithrum, proximal radials, and other regions was completed.

3.3.2. *Development of the Dorsal Fin.* In EFT, at 8 DAH (Figure 11(a)), the second dorsal spine and its fin bones appeared. At 11 DAH (Figure 11(b)), the first dorsal spine and fin bone appeared, the second dorsal spine began to elongate continuously, and barbs appeared. At 17 DAH

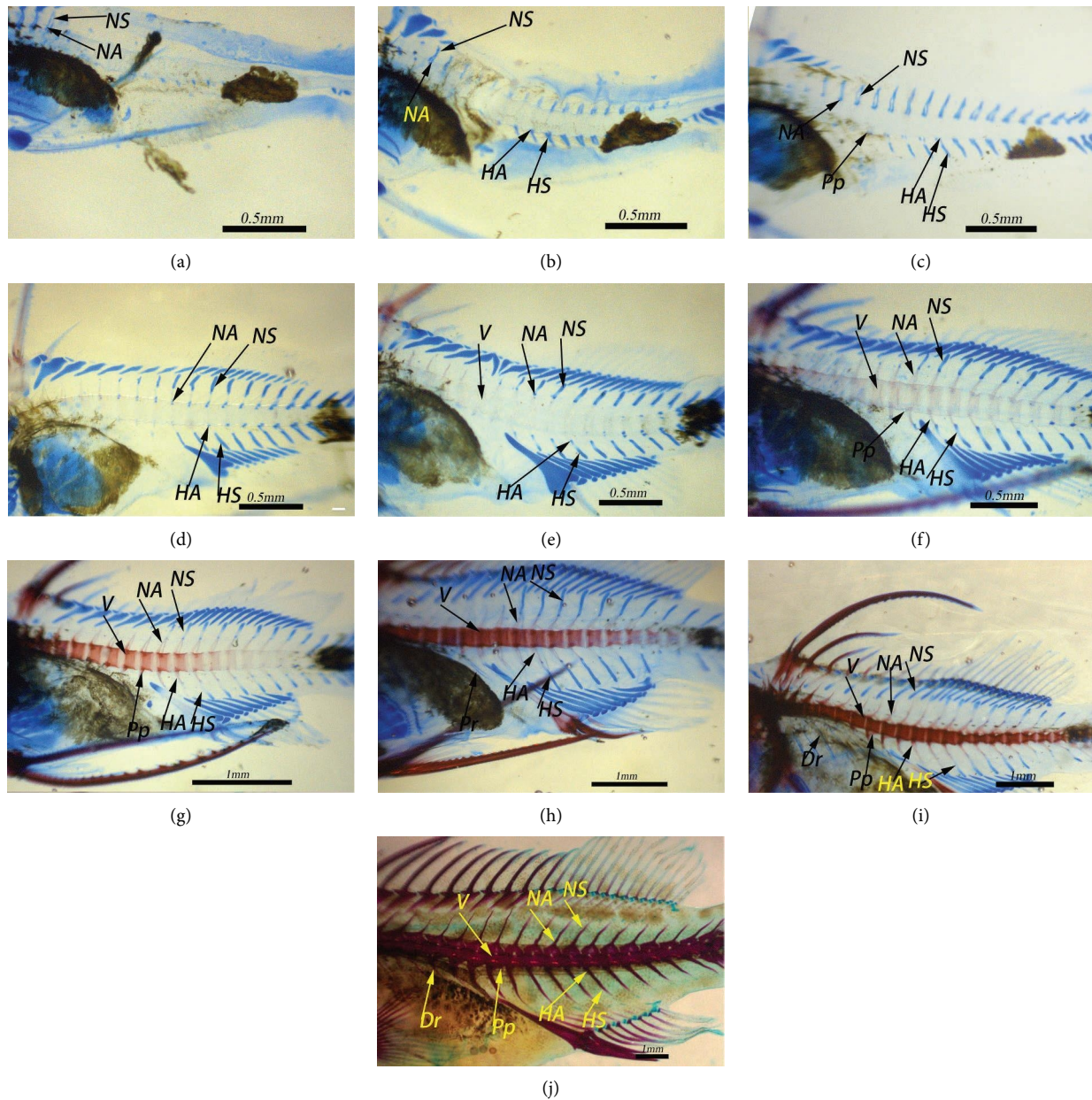


FIGURE 8: Vertebral column development of *E. fuscoguttatus*. (a) 11 DAH (4.21 ± 0.40 mm TL); (b) 14 DAH ($TL 4.76 \pm 0.28$ mm); (c) 17 DAH (6.00 ± 0.47 mm TL); (d) 17 DAH (6.00 ± 0.47 mm TL); (e) 20 DAH (6.85 ± 0.59 mm TL); (f) 23 DAH (7.59 ± 0.46 mm TL); (g) 26 DAH (8.07 ± 1.08 mm TL); (h) 29 DAH (9.99 ± 2.46 mm TL); (i) 32 DAH (12.38 ± 1.53 mm TL); (j) 38 DAH (19.18 ± 1.39 mm TL). Abbreviations are as follows: Dr: dorsal rib; HS: heamal spine; HA: heamal arch; NA: neural arch; NS: neural spine; Pp: parapophysis; Pr: pleural rib; V: vertebral centra.

(Figure 11(d)), the third dorsal spine and fin bone were visible and the first dorsal spine and second dorsal spine began to ossify. At 23 DAH (Figure 11(f)), the fourth dorsal spine developed. At 26 DAH (Figure 11(g)), the rest of the dorsal spines, dorsal fin strips, and dorsal fin distal radials were observed, while the second dorsal fin spine underwent

a degenerative process, gradually shortening. At 32 DAH (Figure 11(i)), stay cartilage appeared. At 38 DAH (Figure 11(j)), the second dorsal spine degenerated and was reduced to the length of the other dorsal spines. The dorsal fin also began to ossify. At 48 DAH (Figure 11(m)), the dorsal fin was completely ossified.

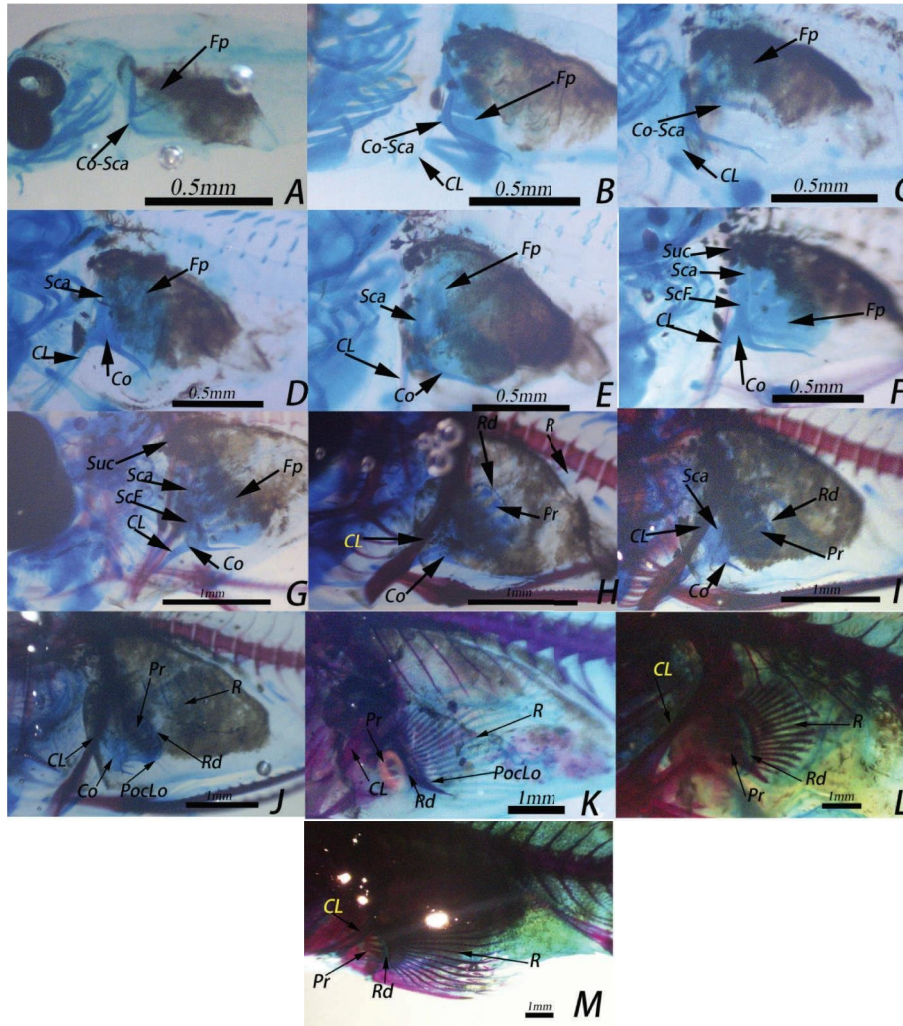


FIGURE 9: Pectoral fin development of EFT. (a) 5 DAH (3.2 ± 0.17 mm TL); (b) 8 DAH (3.97 ± 0.4 mm TL); (c) 11 DAH (4.43 ± 0.41 mm TL); (d) 14 DAH (5.04 ± 0.77 mm TL); (e) 17 DAH (5.61 ± 0.41 mm TL); (f) 20 DAH (6.45 ± 0.48 mm TL); (g) 23 DAH (6.53 ± 0.63 mm TL); (h) 26 DAH (8.34 ± 0.44 mm TL); (i) 29 DAH (8.40 ± 1.2 mm TL); (j) 32 DAH (10.87 ± 1.49 mm TL); (k) 38 DAH (19.18 ± 1.40 mm TL); (l) 43 DAH (27.21 ± 4.6 mm TL); (m) 48 DAH (31.09 ± 2.15 mm TL). Abbreviations are as follows: CL, cleithrum; Co-Sca: coracoid-scapula; Co, coracoid; PocLo, metacleithrum lower; Fp, fin plate; ScF, scapular foramen; Sca, scapula; R, lepidotrichium; Rd, distal radial; Prx, proximal pterygiophore; Suc, hypercleithrum.

In *E. fuscoguttatus*, at 8–17 DAH (Figures 12(b)–12(e)), the degree of development was comparable to that of EFT. At 20 DAH (Figure 12(e)), the rest of the dorsal spines, dorsal fin strips, and distal radius of the dorsal fin were visible, and the second dorsal spine degenerated. At 23 DAH (Figure 12(f)), the stay cartilage was visible. At 43 DAH (Figure 12(k)), the second dorsal spine was shortened to the length of other dorsal spines, slightly longer than the first dorsal spine. The dorsal fin spine also began to ossify.

3.3.3. Development of the Pelvic Fin. In EFT, at 8 DAH (Figure 13(a)), the abdominal spines and fin-based cartilage emerged. At 14 DAH (Figure 13(c)),

abdominal spines were elongated, accompanied by barb growth. At 17 DAH, abdominal spines began to ossify. At 23 DAH (Figure 13(f)), ventral fin development was observed. At 26 DAH (Figure 13(g)), fin-based cartilage ossification was observed. Abdominal spines began to shorten until they were comparable in length to other fin spines.

In *E. fuscoguttatus*, at 8–14 DAH, development was similar to that in EFT. At 17 DAH (Figure 14(c)), the abdominal spines began to ossify, and ventral fin development was observed. At 20 DAH (Figure 14(d)), the basipterygia began to ossify, and the abdominal spine underwent a degenerative shortening process until it was comparable in length to those of other fin spines.

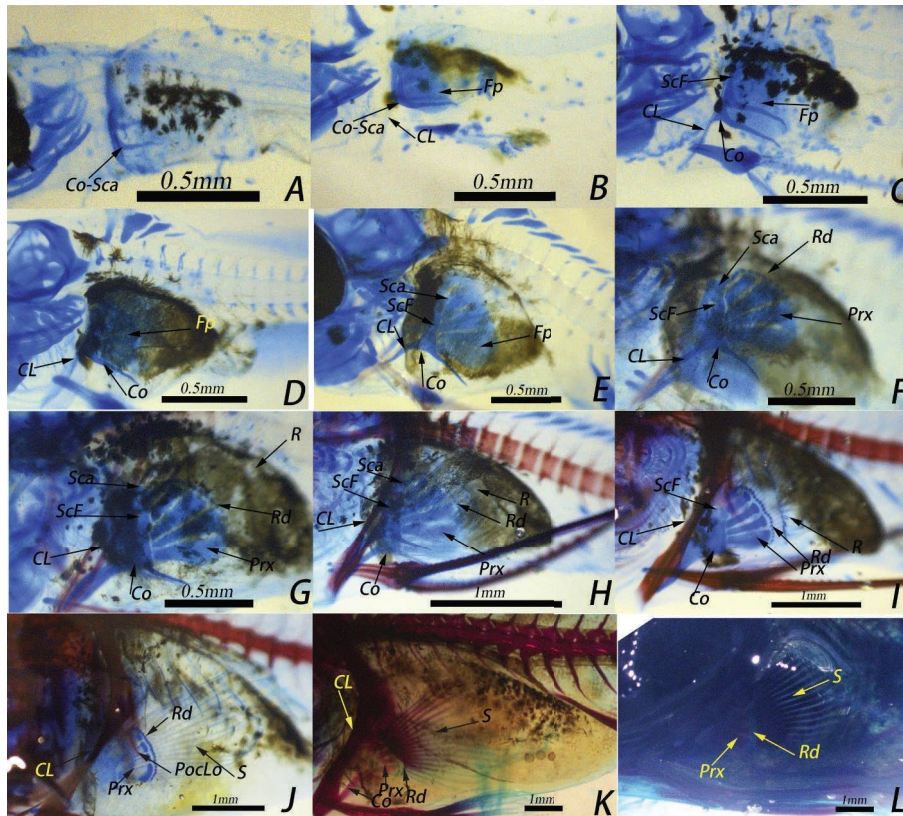


FIGURE 10: Pectoral fin development of *E. fuscoguttatus*. (a) 5 DAH (3.21 ± 0.37 mm TL); (b) 8 DAH (3.61 ± 0.22 mm TL); (c) 11 DAH (4.21 ± 0.40 mm TL); (d) 14 DAH (4.76 ± 0.28 mm TL); (e) 17 DAH (6.00 ± 0.47 mm TL); (f) 20 DAH (6.85 ± 0.59 mm TL); (g) 23 DAH (7.59 ± 0.46 mm TL); (h) 26 DAH (8.07 ± 1.08 mm TL); (i) 29 DAH (9.99 ± 2.46 mm TL); (j) 32 DAH (12.38 ± 1.53 mm TL); (k) 38 DAH (25.16 ± 2.19 mm TL); (l) 43 DAH (30.49 ± 3.16 mm TL). Abbreviations are as follows: CL, cleithrum; Co-Sca, coracoid-scapula; Co, coracoid; PocLo, metacleithrum lower; Fp, fin plate; ScF, scapular foramen; Sca, scapula; R, lepidotrichium; Rd, distal radial; Prx, proximal pterygiophore; Suc, hypercleithrum.

3.3.4. Development of the Anal Fin. In EFT, at 11 DAH (Figure 15(a)), proximal radials appeared, developing from the front of the body to the tail. At 20 DAH (Figure 15(d)), 10 pieces of proximal radials developed, with visible lepidotrichia. At 23 DAH (Figure 15(e)), the distal radials developed. At 26 DAH (Figure 15(f)), the first and second fin spines were visible and began to ossify, and stay cartilage appeared. At 32 DAH (Figure 15(h)), ossification of other spines and basipterygia began. At 43 DAH (Figure 15(j)), ossification was completed.

In *E. fuscoguttatus*, at 17 DAH (Figure 16(b)), proximal radials developed. At 20 DAH (Figure 17(c)), the first and second fin spines, distal radials, anal fin spines, and stay cartilage were visible. At 29 DAH (Figure 16(g)), the first and

second fin spines began to ossify. At 32 DAH (Figure 16(h)), other spines and pterygiophore began to ossify.

3.3.5. Development of the Caudal Fin. In EFT, at 8 DAH (Figure 17(a)), hypural 1 formed. At 11 DAH (Figure 17(b)), hypural 2-3 and parhypural formed. At 17 DAH (Figure 17(d)), parhypural 1-3 formed and caudal fin rays were somewhat visible. At 26 DAH (Figure 17(g)), hypural 4 developed. At 29 DAH (Figure 17(h)), epural 3 and epural 4 fused into a single piece and the caudal fin ray and urostyle started to ossify. At 38 DAH (Figure 17(j)), urostyle osteosis was completed. At 48 DAH (Figure 17(k)), caudal fin ray ossification was nearly complete.

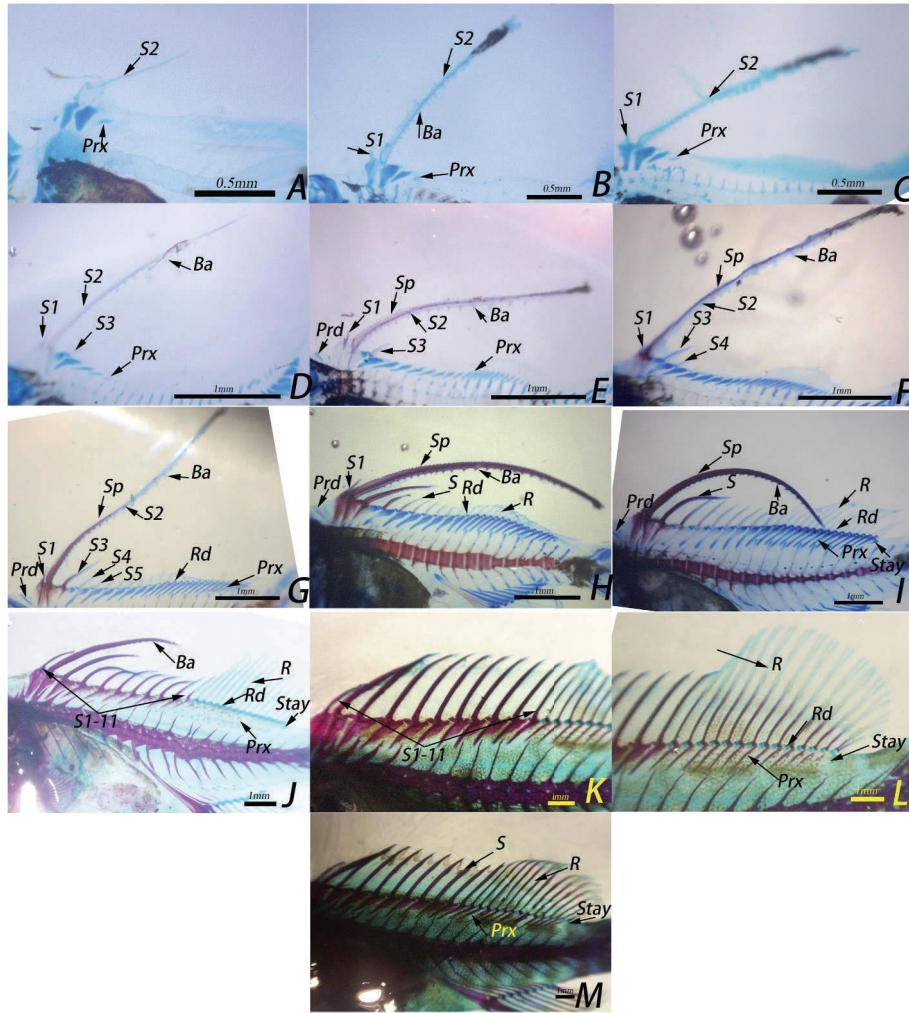


FIGURE 11: Dorsal fin development of EFT. (a) 8 DAH (3.97 ± 0.4 mm TL); (b) 11 DAH (4.43 ± 0.41 mm TL); (c) 14 DAH (5.04 ± 0.77 mm TL); (d) 17 DAH (5.61 ± 0.41 mm TL); (e) 20 DAH (6.45 ± 0.48 mm TL); (f) 23 DAH (6.53 ± 0.63 mm TL); (g) 26 DAH (8.34 ± 0.44 mm TL); (h) 29 DAH (8.40 ± 1.2 mm TL); (i) 32 DAH (10.87 ± 1.49 mm TL); (j) 38 DAH (19.18 ± 1.40 mm TL); (k) 43 DAH (27.21 ± 4.6 mm TL); (l) 43 DAH (27.21 ± 4.6 mm TL); (m) 48 DAH (31.09 ± 2.15 mm TL). Abbreviations are as follows: Ba, barb; Prd, predosal; R, lepidotrichium; Rd, distal radial; S, hard spine; Sp, spinule; stay.

In *E. fuscoguttatus*, at 8 DAH (Figure 18(a)), hypural 1-2 formation was observed. At 11–14 DAH (Figures 18(b) and 18(c)), hypural 3 and parhypural formed. At 17 DAH

(Figure 18(d)), epural 1–3 developed. At 20 DAH (Figure 18(f)), epural 4–5 and hypural 4–5 formed; at the same time, caudal fin rays could be seen. At 29 DAH

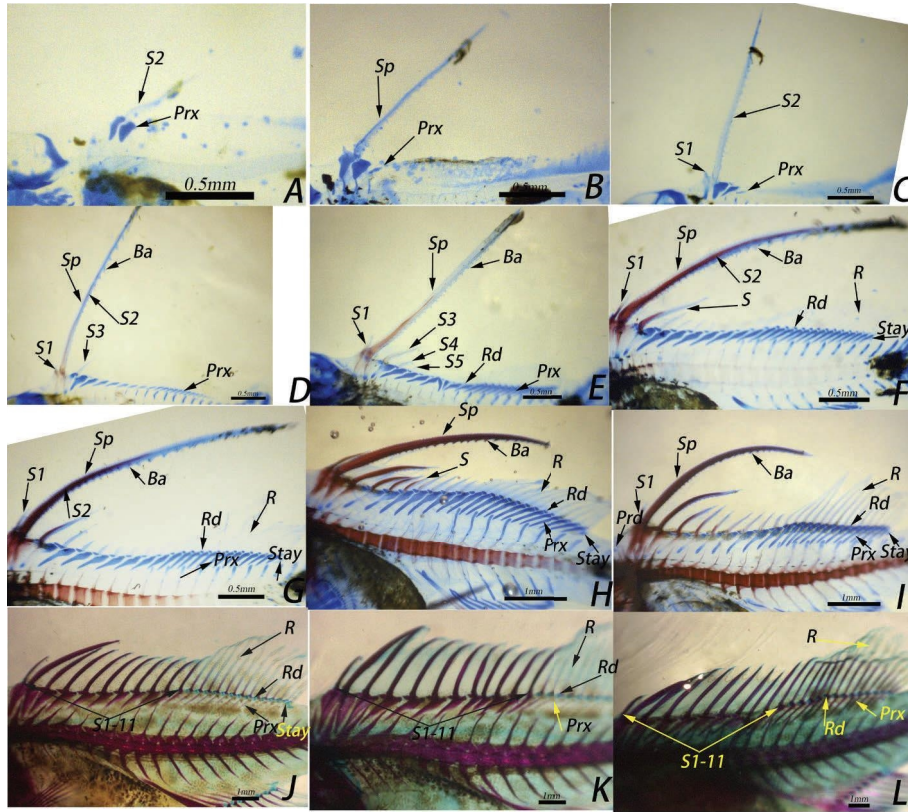


FIGURE 12: Dorsal fin development of *E. fuscoguttatus*. (a) 8 DAH (3.61 ± 0.22 mm TL); (b) 11 DAH (4.21 ± 0.40 mm TL); (c) 14 DAH (4.76 ± 0.28 mm TL); (d) 17 DAH (6.00 ± 0.47 mm TL); (e) 20 DAH (6.85 ± 0.59 mm TL); (f) 23 DAH (7.59 ± 0.46 mm TL); (g) 26 DAH (8.07 ± 1.08 mm TL); (h) 29 DAH (9.99 ± 2.46 mm TL); (i) 32 DAH (12.38 ± 1.53 mm TL); (j) 38 DAH (25.16 ± 2.19 mm TL); (k) 43 DAH (30.49 ± 3.16 mm TL). (l) 48 DAH (37.69 ± 4.58 mm TL). Abbreviations are as follows: Ba, barb; Prd, predorsal; R, lepidotrichium; Rd, distal radial; S, hard spine; Sp, spinule; stay.

(Figure 18(i)), epural 4-5 fused into a single piece, and the urostyle and caudal fin rays began to ossify. At 38 DAH (Figure 18(k)), urostyle ossification was completed. By 48 DAH (Figure 18(l)), ossification of the caudal fin rays was still incomplete.

4. Discussion

4.1. Postembryonic Development of EFT and *E. fuscoguttatus*. Recently, to improve grouper germplasm and obtain groupers with economic traits, hybrid breeding has been widely used. Many hybrid groupers have been reported, such

as *E. lanceolatus* (♂) × *E. brumenus* (♀) [10], *E. lanceolatus* (♂) × *E. moara* (♀) [11], *E. moara* (♀) × *E. akaara* (♂) [12], *E. fuscoguttatus* (♀) × *E. lanceolatus* (♂) [13], *E. moara* (♀) × *E. septemfasciatus* (♂) [14], and *E. fuscoguttatus* (♀) × *E. polyphemadion* (♂) [15]. The main hybrids used for production are *E. lanceolatus* (♂) × *E. moara* (♀) and *E. fuscoguttatus* (♀) × *E. lanceolatus* (♂). At 2–20 DAH, there was no difference in the total length of EFT and *E. fuscoguttatus*. At 23 DAH, *E. fuscoguttatus* larval survival was low. This low survival was not observed in EFT under the same breeding conditions, suggesting that the *E. fuscoguttatus* was affected by the disease, and surviving fry

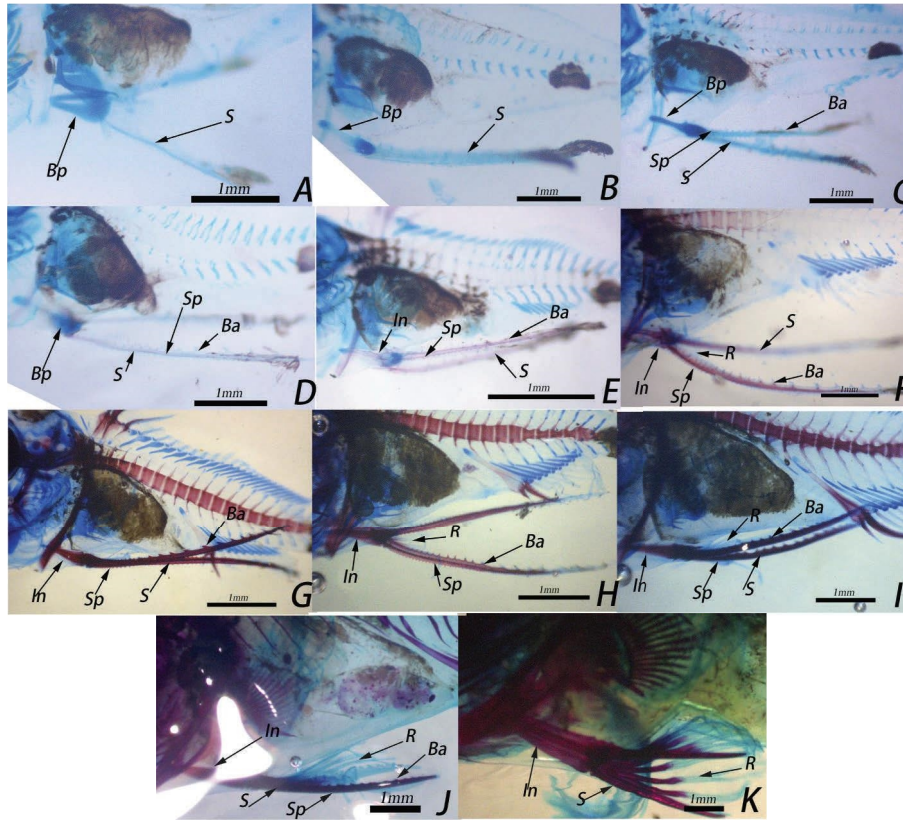


FIGURE 13: Pelvic fin development of EFT. (a) 8 DAH (3.97 ± 0.4 mm TL); (b) 11 DAH (4.43 ± 0.41 mm TL); (c) 14 DAH (5.04 ± 0.77 mm TL); (d) 17 DAH (5.61 ± 0.41 mm TL); (e) 20 DAH (6.45 ± 0.48 mm TL); (f) 23 DAH (6.53 ± 0.63 mm TL); (g) 26 DAH (8.34 ± 0.44 mm TL); (h) 29 DAH (8.40 ± 1.2 mm TL); (i) 32 DAH (10.87 ± 1.49 mm TL); (j) 38 DAH (19.18 ± 1.40 mm TL); (k) 43 DAH (27.21 ± 4.6 mm TL). Abbreviations are as follows: Bp, basipterygium; Bb, barb; R, lepidotrichium S, hard spine; Sp, spinule; In, innominatum.

had strong disease resistance. Subsequent cannibalism resulted in the rapid growth of *E. fuscoguttatus*, resulting in a longer total length than that of EFT. However, at 3 months after hatching, the total length of EFT exceeded that of *E. fuscoguttatus*, and at 4 months after hatching, the total length of EFT was significantly longer than that of *E. fuscoguttatus*. The weight of EFT at this point was 32.7 ± 5.07 g, while that of *E. fuscoguttatus* was 29.7 ± 6.26 g. These results show that EFT grew faster than their female parents, and the mortality rate during growth was lower than that of *E. fuscoguttatus*.

4.2. Skeletal Development of EFT and *E. fuscoguttatus*

4.2.1. Axial Skeletal Development. The skeletal development of fish is closely related to the functional needs of juveniles at different stages, and the prioritization of bone development is related to the survival needs of different periods [16, 17]. During the larval period, the larvae had oral fissures; at this stage, breathing and feeding abilities were crucial and the skeletal features associated with food ingestion and respiration showed preferential development. The cranium developed first in both *E. fuscoguttatus* and EFT, with similar

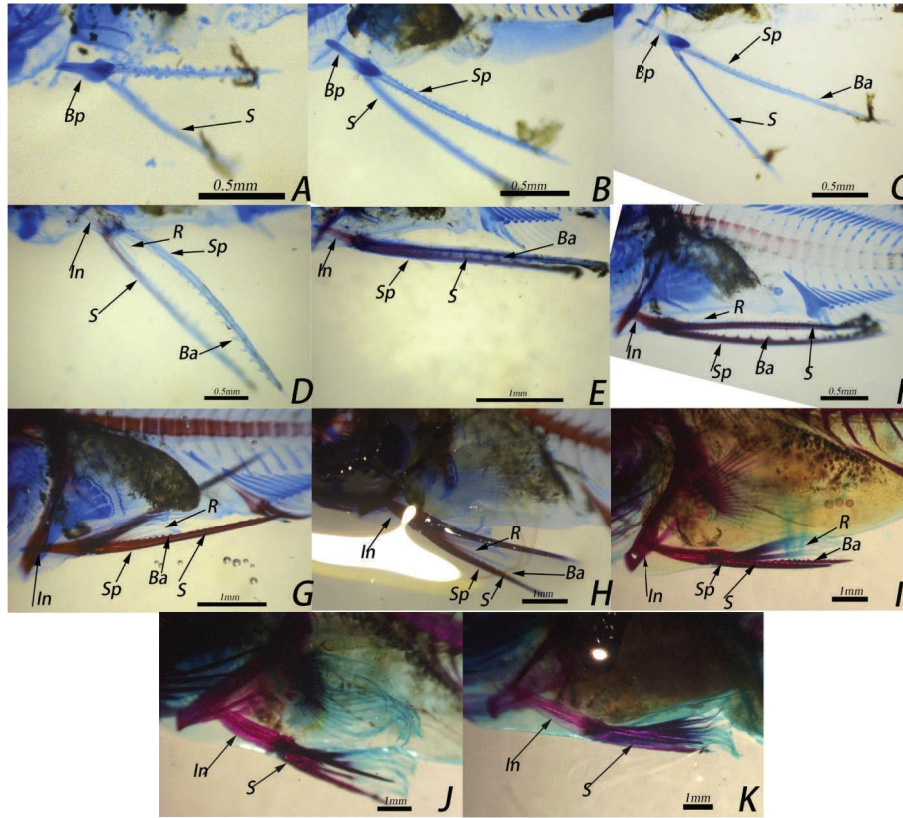


FIGURE 14: Pelvic fin development of *E. fuscoguttatus*. (a) 11 DAH (4.21 ± 0.40 mm TL); (b) 14 DAH (4.76 ± 0.28 mm TL); (c) 17 DAH (6.00 ± 0.47 mm TL); (d) 20 DAH (6.85 ± 0.59 mm TL); (e) 23 DAH (7.59 ± 0.46 mm TL); (f) 26 DAH (8.07 ± 1.08 mm TL); (g) 29 DAH (9.99 ± 2.46 mm TL); (h) 32 DAH (12.38 ± 1.53 mm TL); (i) 38 DAH (25.16 ± 2.19 mm TL); (j) 43 DAH (27.21 ± 4.6 mm TL); (k) 48 DAH (37.69 ± 4.58 mm TL). Abbreviations are as follows: Bp, basipterygium; Bb, barb; R, lepidotrichium S, hard spine; Sp, spinule; In, innominatum.

rates of development, enabling larval respiration and feeding. The ossification of the maxilla, premaxilla, and preopercle occurred before that of other bones of the head. A similar pattern has been discovered in *E. lanceolatus* [18] and *E. akaara* [19].

The vertebral column of a fish is the main support structure in the fish body, usually consisting of the vertebral centrum, neural arch, neural spine, hemal arch, hemal spine, parapophysis, and ribs. Vertebral ossification differs among fish. The development of the vertebral column proceeds

from the head to tail in *Sebastiscus marmoratus* [20], *Larimichthys crocea* [6], and *Rachycentron canadum* [21] and from the head to tail to middle portion of *Alosa sapidissima* [22]. Spine ossification in *E. fuscoguttatus* and EFT also occurred from the head to tail.

4.2.2. Appendage Skeletal Development. The pectoral fins are the only fins that exist before larvae open their mouths to feed in various species, such as *Scyliorhinus canicula* and *Pagellus erythrinus* [23]. In this study, the pectoral fin

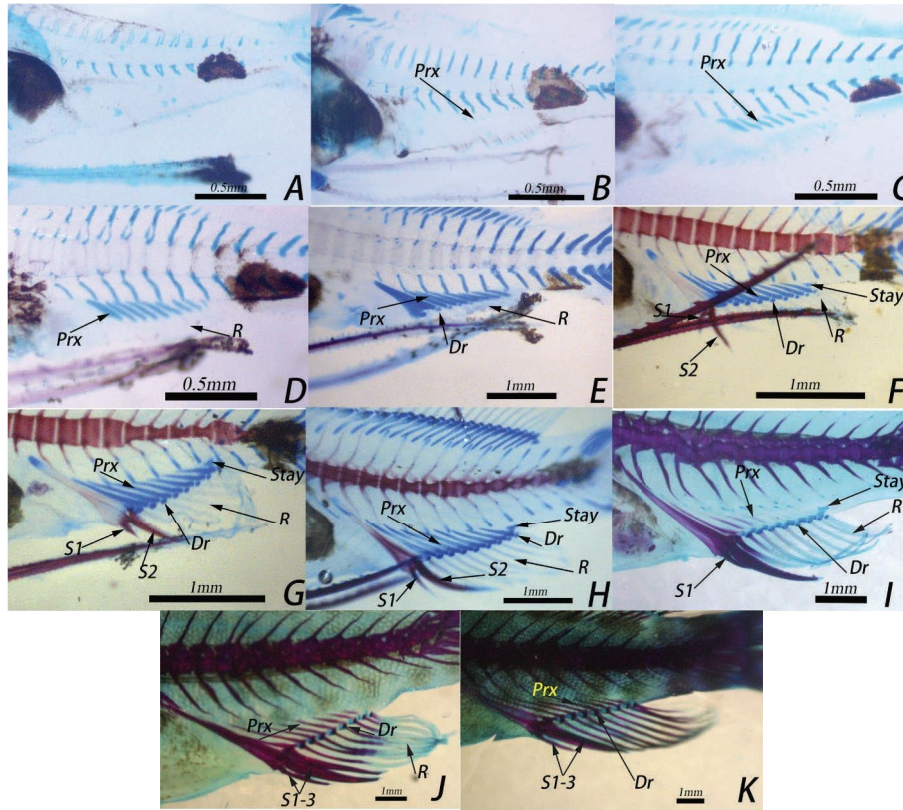


FIGURE 15: Anal fin development of EFT. (a) 11 DAH (4.43 ± 0.41 mm TL); (b) 14 DAH (5.04 ± 0.77 mm TL); (c) 17 DAH (5.61 ± 0.41 mm TL); (d) 20 DAH (6.45 ± 0.48 mm TL); (e) 23 DAH (6.53 ± 0.63 mm TL); (f) 26 DAH (8.34 ± 0.44 mm TL); (g) 29 DAH (8.40 ± 1.2 mm TL); (h) 32 DAH (10.87 ± 1.49 mm TL); (i) 38 DAH (19.18 ± 1.40 mm TL); (j) 43 DAH (27.21 ± 4.6 mm TL); (k) 48 DAH (31.09 ± 2.15 mm TL). Abbreviations are as follows: Dr, distal radial; R, lepidotrichium; S, hard spine; Prx, proximal radial; stay.

was indeed the first appendage to develop in *E. fuscoguttatus* and EFT, as observed in *E. lanceolatus* [24] and *E. awoara* (♀) × *E. tukula* (♂) [25]. Early development of the pectoral fin may enable simple swimming in the early larval period.

During the development of groupers, the dorsal fin spines and ventral fin spines lengthen and contract substantially; this is a special feature of grouper development [26]. This feature is also often used to divide groupers into larval and juvenile stages [27, 28].

In *Hexagrammos otakii* [29] and *Chaeturichthys stigmatia* [30], the dorsal fin and pelvic fins develop after the

pectoral and caudal fins. Dorsal and pelvic fins developed earlier than caudal fins in EFT and *E. fuscoguttatus*, similar to the developmental sequence in *E. fuscoguttatus* (♀) × *E. lanceolatus* (♂) [13] and *E. lanceolatus* [31]. During the larval stage, the elongation of the second dorsal fin spine and pelvic fin spine, usually in a natural open state, helps larvae to maintain body stability in the current. The second dorsal fin spine of EFT began to degenerate at 26 DAH, which is later than the corresponding time point in *E. fuscoguttatus* (20 DAH), enabling EFT to swim stably during the growth process, thereby improving survival. The dorsal fin spines of

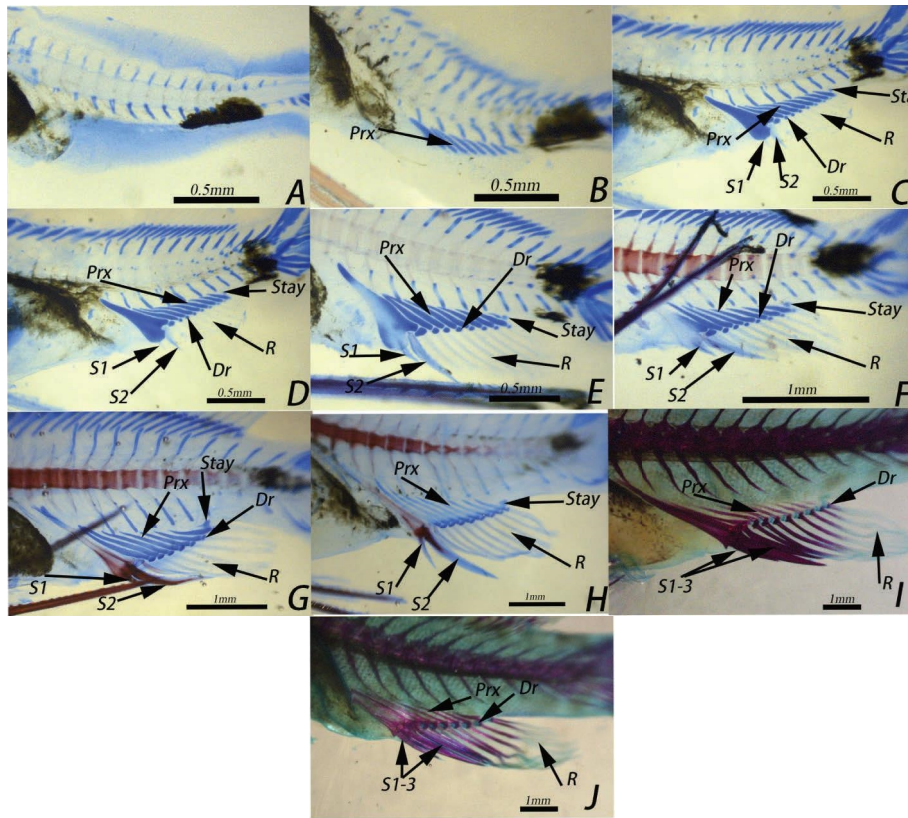


FIGURE 16: Anal fin development of *E. fuscoguttatus*. (a) 14 DAH (TL 4.76 ± 0.28 mm); (b) 17 DAH (6.00 \pm 0.47 mm TL); (c) 20 DAH (6.85 \pm 0.59 mm TL); (d) 20 DAH (6.85 \pm 0.59 mm TL); (e) 23 DAH (7.59 \pm 0.46 mm TL); (f) 26 DAH (8.07 \pm 1.08 mm TL); (g) 29 DAH (9.99 \pm 2.46 mm TL); (h) 32 DAH (12.38 \pm 1.53 mm TL); (i) 38 DAH (25.16 \pm 2.19 mm TL); (j) 48 DAH (37.69 \pm 4.58 mm TL). Abbreviations are as follows: Dr, distal radial; R, lepidotrichium; S, hard spine; Prx, proximal radial; stay.

EFT shrink less than those of *E. fuscoguttatus*, further indicating that EFT can undergo a rapid metamorphosis.

The anal fin functions in the maintenance of balance, preventing tilting and rocking, and coordinating swimming. The caudal fin is an important driving organ of the fish, providing power for the fish body to swim forward, and the caudal fin contributes to the swimming direction. The anal fin and caudal fin of EFT had shorter ossification times than those in *E. fuscoguttatus*, suggesting that EFT had an advantage with respect to swimming and enemy avoidance. There is a fusion of the hypural and epural during the development of the caudal fin. The hypural of *Hexagrammos otakii* [29] and *Favonigobius gymnauchen* [32] fuse. This fusion may promote a stronger tail thrust,

thereby improving the ability to catch prey and avoid predators. In this study, both *E. fuscoguttatus* and EFT had epural fusion. After the fusion of the caudal bones in EFT, there were three epural bones, as observed in most groups, while *E. fuscoguttatus* had four epural bones when the ossification of the caudal fin was completed. In addition, *Salanx ariakensis* [33] and *Solea senegalensis* [34] have one epural bone, *Thunnus tonggol* [35] has four epural bones, *Siniperca chuatsi* [36] has three epural bones, *E. awoara* [37] has three epural bones, and *Takifugu flavidus* [38] has no epural bone. At present, there are no reports on the function of the epural, and further research is needed to evaluate the number of epural bones and the functional significance of fusion.

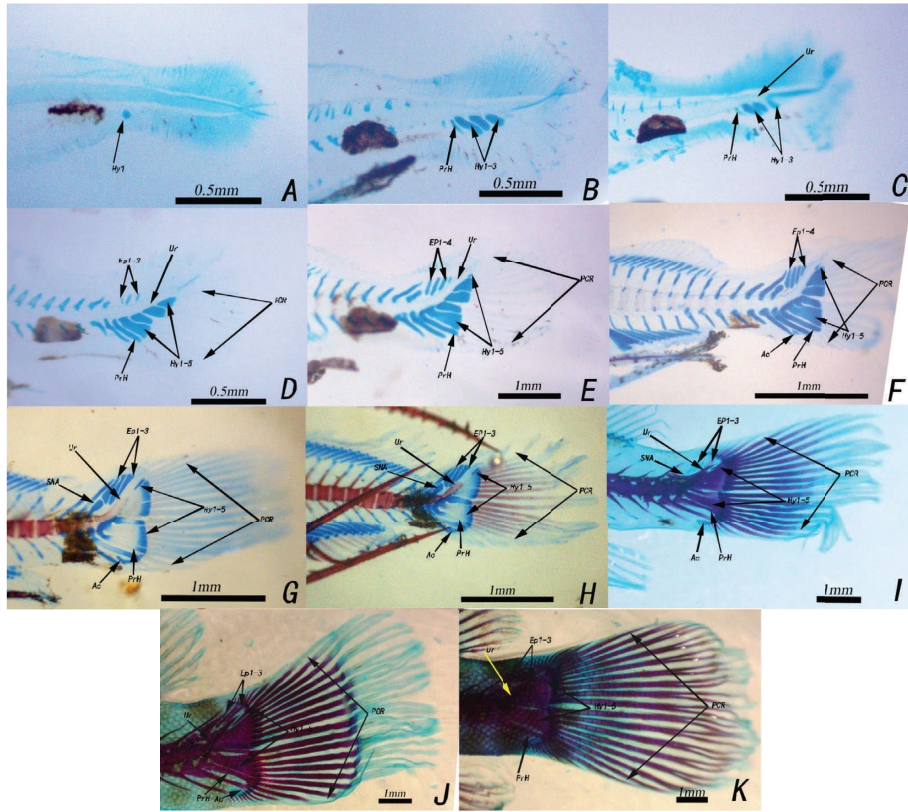


FIGURE 17: Caudal fin development of EFT. (a) 8 DAH (3.97 ± 0.4 mm TL); (b) 11 DAH (4.43 ± 0.41 mm TL); (c) 14 DAH (5.04 ± 0.77 mm TL); (d) 17 DAH (5.61 ± 0.41 mm TL); (e) 20 DAH (6.45 ± 0.48 mm TL); (f) 23 DAH (6.53 ± 0.63 mm TL); (g) 26 DAH (8.34 ± 0.44 mm TL); (h) 29 DAH (8.40 ± 1.2 mm TL); (i) 32 DAH (10.87 ± 1.49 mm TL); (j) 38 DAH (19.18 ± 1.40 mm TL); (k) 43 DAH (27.21 ± 4.6 mm TL). Abbreviations are as follows: Ac, accessory; Ep, epural; Hy, hypural; PCR, caudal lepidotrichia; PrH, parhyural; SNA, specialized neural; Ur, urostyle.

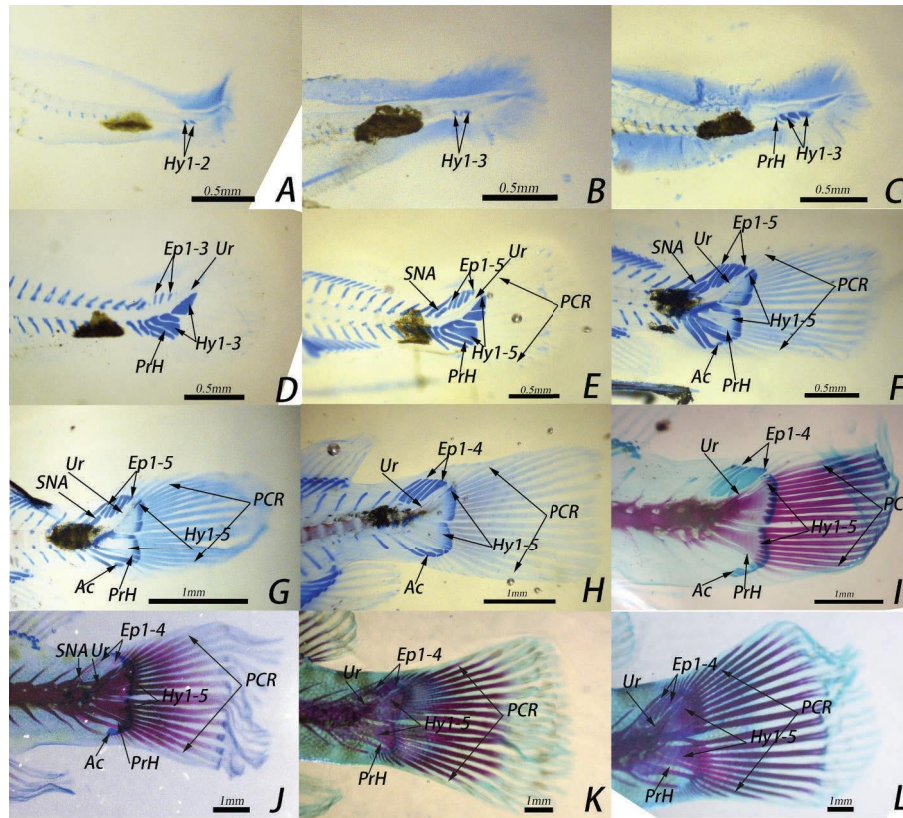


FIGURE 18: Caudal fin development of *E. fuscoguttatus*. (a) 8 DAH (3.61 ± 0.22 mm TL); (b) 11 DAH (4.21 ± 0.40 mm TL); (c) 14 DAH (4.76 ± 0.28 mm TL); (d) 17 DAH (6.00 ± 0.47 mm TL); (e) 17 DAH (6.00 ± 0.47 mm TL); (f) 20 DAH (6.85 ± 0.59 mm TL); (g) 23 DAH (7.59 ± 0.46 mm TL); (h) 26 DAH (8.07 ± 1.08 mm TL); (i) 29 DAH (9.99 ± 2.46 mm TL); (j) 32 DAH (12.38 ± 1.53 mm TL); (k) 38 DAH (25.16 ± 2.19 mm TL); (l) 48 DAH (37.69 ± 4.58 mm TL). Abbreviations are as follows: Ac, accessory; Ep, epural; Hy, hypural; PCR, caudal lepidotrichia; PrH, parhyural; SNA, specialized neural; Ur, urostyle.

5. Conclusion

In this study, the postembryonic development and skeletal development of *E. fuscoguttatus* and the hybrid EFT were observed, revealing that the development of EFT lagged behind that of *E. fuscoguttatus* slightly in the larval and juvenile stages, while the growth rate of EFT was faster than that of *E. fuscoguttatus* in the juvenile stage, indicating that EFT had a growth advantage. The order of skeletal development was similar in EFT and *E. fuscoguttatus*, indicating that skeletal development in EFT was normal. In addition, compared with that morphology of other groupers, *E. fuscoguttatus* had an extra epural bone; the molecular mechanism and significance of this extra bone remain to be explored.

Data Availability

The data used to support the findings of this study are included within the article.

Conflicts of Interest

The authors declare that there are no conflicts of interest.

Acknowledgments

The research project was partially (or fully) sponsored by the Taishan Industry Leading Talent Project (Grant no. LJNY202109), China Agriculture Research System of MOF and MARA (CARS-47), Breeding Project of Shandong Province (Grant no. 2019LZGC020), The Central Public-interest Scientific Institute Basal Research Fund, CAFS (Grant nos. 2020XT06, 2020TD19, and 2020TD25), and Yellow Sea Fisheries Research Institute Research Fees (Grant nos. 20603022019002 and 20603022020015).

References

- [1] Y. S. Tian, J. Tang, W. H. Ma et al., "Development and growth of hybrid offspring of brown grouper *Epinephelus fuscoguttatus*(♀) × blue speckled grouper *Epinephelus tukula*(♂) using cryopreserved sperm," *Program Fisheries Science*, vol. 40, pp. 36–47, 2019.
- [2] Y. P. Wu, Y. S. Tian, Z. T. Li et al., "Analysis on morphological difference between hybrid *Epinephelus fuscoguttatus* ♀ × *E. tukula* ♂ and its parents," *J. Guangdong Ocean University*, vol. 39, pp. 17–22, 2019.
- [3] Y. P. Wu, Y. S. Tian, L. N. Wang et al., "Genetic diversity analysis of *Epinephelus fuscoguttatus*(♀) and *E. tukula*(♂) hybrids," *Program Fisheries Science*, vol. 42, pp. 25–32, 2021b.

- [4] P. F. Duan, Y. S. Tian, Z. T. Li et al., "Hypoxia tolerance of *Epinephelus fuscoguttatus*(♀)×*E. tukula*(♂) hybrids and *E. fuscoguttatus*," *Journal of Fishery Sciences of China*, vol. 29, pp. 220–233, 2022.
- [5] Y. P. Wu, Y. S. Tian, Z. T. Li et al., "Karyotype analysis of hybrids of *Epinephelus fuscoguttatus*(♀)×*Epinephelus tukula*(♂)," *J. Guangdong Ocean University*, vol. 41, pp. 119–123, 2021a.
- [6] W. Q. Huang, Y. Zhang, F. F. Zhou et al., "Spinal vertebrae of a large yellow croaker (*Larimichthys crocea*) along with its early development," *Marine Science*, vol. 45, pp. 51–58, 2021.
- [7] X. J. Lv, S. H. Xu, Q. H. Liu et al., "Osteological ontogeny and allometric growth in larval and juvenile turbot (*Scophthalmus maximus*)," *Aquaculture*, vol. 498, pp. 351–363, 2019.
- [8] G. Dingerkus and L. D. Uhler, "Enzyme clearing of alcian blue stained whole small vertebrates for demonstration of cartilage," *Stain Technology*, vol. 52, no. 4, pp. 229–232, 1977.
- [9] W. R. Taylor and G. C. Vandyke, "Revised procedures for staining and clearing small fishes and other vertebrates for bone and cartilage study," *Cybium*, vol. 9, no. 2, pp. 107–119, 1985.
- [10] Y. P. Wu, Y. S. Tian, M. L. Cheng et al., "Comparison of metamorphosis development and growth of hybrid offspring of *Epinephelus lanceolatus*(♂) and *E. bruneus*(♀) or *E. moara*(♀)," *Program Fisheries Science*, vol. 41, pp. 23–32, 2020.
- [11] S. Q. Wu, L. Y. Zheng, Z. C. Huang et al., "Embryonic and morphological development in larva, juvenile, and young stages of hybrid grouper(*Epinephelus moara* ♀×*E.lanceolatus* ♂)," *Program Fisheries Science*, vol. 38, pp. 27–35, 2016.
- [12] Q. H. Yang, Z. C. Huang, L. Y. Zheng, L. B. Li, Y. H. Liu, and Z. H. Xu, "Embryonic development and growth of hybrid from the hybridization of *Epinephelus moara*(♀) ×," *E. akaara*(♂) *Mar. Fisheries*, vol. 36, pp. 224–231, 2014.
- [13] C. Chen, X. D. Kong, Y. L. Li et al., "Embryonic and morphological development in the larva, juvenile, and young stages of *Epinephelus fuscoguttatus*(♀)×*E. lanceolatus*(♂)," *Program Fisheries Science*, vol. 35, pp. 135–144, 2014.
- [14] Y. L. Li, Q. Y. Wang, C. Chen et al., "Embryonic and morphological development in larva, juvenile, and young stages of F1 by *Epinephelus moara*(♀)×," *Journal of Fishery Sciences of China*(♂), vol. 19, no. 5, pp. 821–832, 2013.
- [15] G. Chen, J. S. Huang, J. D. Zhang, Z. L. Wang, B. G. Tang, and C. H. Pan, "Feeding habits and growth characteristics of larvae and juvenile hybrid grouper (*Epinephelus fuscoguttatus*♀×*E. polyphemus*♂)," *Journal of Fisheries of China*, vol. 42, pp. 1766–1777, 2018.
- [16] L. A. Fuiman, "Growth gradients in fish larvae," *Journal of Fish Biology*, vol. 23, no. 1, pp. 117–123, 1983.
- [17] J. W. M. Osse, J. van den Boogaart, G. van Snik, and L. van der Sluys, "Priorities during early growth of fish larvae," *Aquaculture*, vol. 155, no. 4, pp. 249–258, 1997.
- [18] X. J. Lv, Y. N. Wang, Q. H. Liu, J. M. Zhai, and J. Li, "Research on skeletal development and allometric growth in larval and juvenile *Epinephelus lanceolatus*," *Marine Science*, vol. 42, pp. 116–121, 2018a.
- [19] J. Y. Park, K. H. Han, J. K. Cho, J. I. Myeong, and J. M. Park, "Early osteological development of larvae and juveniles in red spotted grouper, *Epinephelus akaara* (pisces: Serranidae)," *Development Reprod.*, vol. 20, no. 2, pp. 87–101, 2016.
- [20] P. P. Deng, Y. L. Yan, and Y. H. Shi, "Early development of the vertebral column and appendicular skeleton in *Sebastiscus marmoratus* larvae," *Journal of Zhejiang University (Science Edition)*, vol. 44, pp. 735–742, 2018.
- [21] F. F. Mao, G. Chen, Q. Ma et al., "Development characteristics of the vertebral column and the appendicular skeleton in larval and juvenile cobia(*Rachycentron canadum*)," *Journal of Fisheries of China*, pp. 1–10, 2023.
- [22] P. P. Deng, Y. H. Shi, J. B. Xu et al., "Early development of the vertebral column and appendicular skeleton of *Alosa sapidissima*," *Journal of Fishery Sciences of China*, vol. 24, no. 1, pp. 73–81, 2017.
- [23] D. G. Sfakianakis, G. Koumoundouros, P. Divanach, and M. Kentouri, "Osteological development of the vertebral column and of the fins in *Pagellus erythrinus* (L. 1758). Temperature effect on the developmental plasticity and morpho-anatomical abnormalities," *Aquaculture*, vol. 232, no. 4, pp. 407–424, 2004.
- [24] L. Zhou, W. M. Weng, J. L. Li, and Q. M. Lai, "Studies on embryonic development, morphological development and feed changeover of *Epinephelus lanceolatus* larva," *Chinese Agricultural Science Bulletin*, vol. 26, pp. 293–302, 2010.
- [25] S. Chen, Y. Tian, Z. Li et al., "Metamorphosis and skeletal development of hybrid *Epinephelus awoara* (♀) and *Epinephelus tukula* (♂) progenies," *Aquaculture*, vol. 530, Article ID 735727, 2021.
- [26] S. X. Ding, Q. H. Liu, H. H. Wu, and M. Qu, "A review of research advances on the biology and artificial breeding of groupers," *Journal of Fishery Sciences of China*, vol. 25, no. 4, pp. 737–752, 2018.
- [27] G. H. Chen and B. Zhang, *Observation on the Morphology of the Larva, Juvenile and Young Fish of Epinephelus malabaricus (Bloch & Schneider)*, pp. 151–156, Natural Science Journal Of Hainan University, 2001.
- [28] Y. H. Liu, Y. Z. Zhang, Y. P. Zhong, J. Li, Y. J. Xie, and J. C. Hu, "Morphological observation on the larva, juvenile and young of *Epinephelus moara*," *Journal of Applied Oceanography*, vol. 35, pp. 514–521, 2016.
- [29] C. Y. Yu, S. G. Guan, D. D. Yu et al., "Development of vertebral column and appendicular skeleton in larvae and juveniles of fat greenling *Hexagrammos otakii*," *Journal of Dalian Ocean University*, vol. 35, pp. 47–55, 2020.
- [30] J. L. Huang, F. Hu, X. J. Song, Y. G. Chen, and J. S. Zhong, "Development of the vertebral column and appendicular skeleton in larvae and juveniles of *Chaeturichthys stigmatias*," *Journal of Shanghai Ocean University*, vol. 31, pp. 71–85, 2022.
- [31] R. X. Guo, S. Y. Fu, W. Yang et al., "Study on the growth and development of larva, juvenile and young fish of *Epinephelus lanceolatus*," *Journal of Aquaculture*, vol. 32, pp. 8–13, 2011.
- [32] D. S. Jin, J. M. Park, J. I. Baek, and K. H. Han, "Osteological development of the larvae and juvenile of *Favonigobius gymnauchen* (Pisces:Gobiidae)," *Dev Reprod.*, vol. 25, no. 1, pp. 33–41, 2021.
- [33] X. D. Wang, M. D. He, J. Zeng, L. F. Li, and J. S. Zhong, "Development of the vertebral column and the appendicular skeleton in the larvae and juveniles of *Salanx ariakensis* in the north of Hangzhou Bay," *Journal of Shanghai Ocean University*, vol. 27, pp. 930–937, 2018.
- [34] P. J. Gavaia, M. T. Dinis, and M. L. Cancela, "Osteological development and abnormalities of the vertebral column and caudal skeleton in larval and juvenile stages of hatchery-reared Senegal sole (*Solea senegalensis*)," *Aquaculture*, vol. 211, no. 4, pp. 305–323, 2002.
- [35] R. Yang, G. Yu, J. Hu, S. J. Zhou, W. Fang, and Z. H. Ma, "Research on skeleton system of *Thunnus tonggol*. South China Fish," *Science*, vol. 17, pp. 36–43, 2021.
- [36] X. Y. Cao, J. L. Zhao, X. W. Chen, H. T. Zhou, Y. Y. Hao, and Y. Zhao, "Early ossification of the skeletal system in larval and

- juvenile *Siniperca chuatsi*,” *Journal of Fishery Sciences of China*, vol. 26, no. 2, pp. 304–313, 2019.
- [37] Q. R. Wang, J. G. Bi, L. M. Lin, and Z. Y. Wang, “Skeletal abnormalities in cultured juvenile yellow grouper *Epinephelus awoara*,” *Journal of Dalian Ocean University*, vol. 27, pp. 417–421, 2012.
- [38] Z. F. Zhang, Y. H. Shi, Y. D. Xie, H. M. Zhang, J. B. Xu, and G. H. Lu, “Early development of the vertebral column, appendicular skeleton and aculeus in the Tawny puffer(*Takifugu flavidus*),” *Journal of Shanghai Ocean University*, vol. 25, pp. 853–865, 2016.